academicJournals

Vol. 8(8), pp. 295-301, 28 February, 2013
DOI: 10.5897/IJPS12.081
ISSN 1992-1950 ©2013 Academic Journals
http://www.academicjournals.org/IJPS

International Journal of Physical Sciences

Full Length Research Paper

Improvement of electromagnetic wave (EMW) shielding through inclusion of electrolytic manganese dioxide in cement and tile-based composites with application for indoor wireless communication systems

Johann Christiaan Pretorius* and B. T. Maharaj

Department of Electrical Electronic and Computer Engineering, University of Pretoria, Pretoria, South Africa.

Accepted 27 February, 2013

The electromagnetic wave absorption characteristics of composite cement-based building material have attracted much interest in recent times. Researchers have mainly focused on the 2 GHz to 12 GHz frequency range while the authors have investigated the mobile and WiFi frequency bands. The determination of characteristics such as reflection loss, absorption, attenuation and shielding effectiveness are crucial in the evaluation and development of these materials for the building industry. The authors have determined the characteristics by measuring the S_{11} and S_{21} parameters of the composite cement-based material in the Global System for Mobile (GSM) and WiFi frequency bands. MnZn-ferrite and electrolytic manganese dioxide in powder form is used as absorber material to increase the permeability of the cement-based material to improve absorption and attenuation capabilities to create a cost-effective practical electromagnetic wave absorber. The results achieved show the uniqueness of electrolytic manganese dioxide as filler in composite cement based material for electromagnetic wave shielding effectiveness improvement. Shielding of 8 dB in the GSM850 and GSM900 frequency bands and 5 dB in the GSM1800 and GSM1900 frequency bands were measured.

Key words: Electromagnetic wave absorption measurement, attenuation, magnetic composites in building material, reflection loss, shielding effectiveness, transmission loss.

INTRODUCTION

The electromagnetic wave (EMW) absorption capability of composite cement-based material has attracted much attention from researchers in recent times. Researchers have adopted various methods to determine the absorption characteristics of such materials.

Absorption is an indication of how much of the EMW energy enters the material. Attenuation indicates how much of the absorbed energy is converted into other forms of energy by the material. The most common method used to determine absorption, is to measure the reflection loss (S11) at the material by placing a conductive back plate behind the device under test (DUT). This is done practically with a vector network analyzer (VNA) and two horn antennae in an anechoic chamber (Guan et al., 2006, 2007). This experimental setup actually measures the total EMW energy attenuated by the material.

Shielding effectiveness (SE) is a combination of reflection loss, attenuation and multiple internal reflections and attenuations (Schulz et al., 1988). SE can be measured by placing the DUT between two horn antennae and measuring the transmission loss (S21)

*Corresponding author. E-mail: pretoriusjc@tut.ac.za. Tel: +27824428946. Fax: +27137453557.

through the material (Park et al., 2006). This method gives an indication of the total shielding effect, but the actual attenuation of the EMW in the material is not available.

In literature and applications, different composite cement-based materials are used to absorb and attenuate EMW energy. Expanded polystyrene is added to cement-based EMW absorber to improve its absorbing properties (Guan et al., 2005, 2007). This method shows that the attenuation is mainly due to multiple internal reflections and scattering. SE of 6 to 16 dB in the 8 to 18 GHz frequency range is measured. Carbon fillers (Guan et al., 2006) in the form of graphite and carbon black are used for shielding and absorption respectively. SE of 5 to 15 dB is achieved in the 2 to 8 GHz frequency range with carbon black.

Ferrite and stainless steel powder can be used as fillers in wood building material for EMW absorption in indoor applications (Oka et al., 2009). Absorption of above 10 dB is measured at frequencies above 2 GHz. However, the cost of these fillings is high and processing is complicated. Research has mainly been done in the 2 GHz to 12 GHz (X-band) frequency range.

In this research, the authors report on research findings to determine the exact absorption and attenuation capabilities of cement-based building material in mobile communications and indoor wireless communication systems. Electrolytic manganese dioxide (EMD) and MnZn-ferrite (CHY13K) are used as novel magnetic powder fillers in cement-based building material, and the enhanced performance of EMD when compared to CHY13K is shown. The measurement techniques in this research determine the absorption, attenuation and SE capabilities of the material. The absorption is determined by using the gating function of a VNA measuring in the time domain. The results of the combination of the two measurement methods enable one to determine the reflection, absorption and attenuation capabilities.

MATERIALS AND METHODS

Preparation of samples

The composite cement-based samples were prepared in square tile format with 300 mm side lengths and a thickness of 20 mm. The mixture for plaster cement is typically one part cement and six parts sifted river sand. The newly developed mixture used is one part cement, x parts river sand and y parts filler powder with x + y = 6. Table 1 shows the detail of the prepared samples. The ferrimagnetic powder CHY13K is $MnZnFe_2O_4$ with an initial relative complex permeability of 13000 H/m. The magnetic powder EMD is MnO_4 produced for alkaline and lithium cylindrical and flat battery cells. These two magnetic powders were chosen as magnetic fillers because of their high complex permeability.

The prepared samples were naturally cured for at least 12 weeks to reduce the moisture content, as moisture increases the conductivity of the material, hence increasing reflection loss and SE (Kharkovsky et al., 2002).

Measurement theory

When a propagating EMW with unit amplitude is perpendicular incident (normal incidence) on an absorbing material with a conductive back plate, the impedance η normal to the material is given by

$$\eta = \eta_1 \frac{\eta_2 + j\eta_1 \tanh \gamma d}{\eta_1 + j\eta_2 \tanh \gamma d} \quad (1)$$

with η_1 the complex intrinsic impedance of the material, η_2 the impedance of material at distance d in the material, and γ the propagation constant (Schulz et al., 1988; Nie et al., 2005; Kim et al., 2004).

The complex intrinsic impedance of the material is

$$\eta_1 = \sqrt{\frac{j\omega\mu}{\sigma + j\omega\varepsilon}} \quad (2)$$

where $\varepsilon = \varepsilon_0\varepsilon_r$ is the complex permittivity, $\mu = \mu_0\mu_r$ is the complex permeability of the material and $\omega = 2\pi f$ is the frequency in radians per second.

The free space permittivity is $\varepsilon_0 = 8.854 \times 10^{-12}$ F/m, $\mu_0 = 4\pi \times 10^{-7}$ H/m is the free space permeability while ε_r and μ_r are the relative complex permittivity and permeability, respectively of the material (Baoyi et al., 2012). The propagation constant γ in the material can be expressed as:

$$\gamma = j\omega\sqrt{\mu\varepsilon}\sqrt{1 \quad j\frac{\sigma}{\omega\varepsilon}} = \alpha + j\beta \quad (3)$$

where α denotes the attenuation constant in nepers per meter and β the phase constant in radians per second of the material. The impedances and propagation constant in Equations (1) to (3) are dependent on the frequency.

The transmission loss T, resulting from both the front and back interfaces and with the successive internal reflections neglected because of very high internal attenuation *(A > 15 dB)*, is the product of the transmission coefficients across the two interfaces. Hence:

$$T = \frac{4\eta_1\eta_0}{(\eta_1+\eta_0)^2}. \quad (4)$$

The wave impedance is $\eta_0 = 120\pi$ for free space. With the internal attenuation less than 15 dB, successive internal reflections and attenuations cannot be neglected and the net transmission loss T becomes:

$$T = \left[\left(\frac{4\eta_1\eta_0}{(\eta_1+\eta_0)^2}\right) / \left(1 - \frac{(\eta_0-\eta_1)^2}{(\eta_0+\eta_1)^2} e^{-2\gamma D}\right)\right] e^{-\gamma D} \quad (5)$$

By definition, the total SE is (Mishra et al., 2013; Hutagalung et al., 2012):

$$\begin{aligned} SE &= A + R + B \\ &= -20log|T| \\ &= 20log|e^{\gamma D}| \\ &-20log\left|\frac{4\eta_1\eta_0}{(\eta_1+\eta_0)^2}\right| \\ &+20log\left|1 - \frac{(\eta_0-\eta_1)^2}{(\eta_0+\eta_1)^2} e^{-2\gamma D}\right| \end{aligned} \quad (6)$$

Equation (6) is the complete formula for SE of a single shield with *A*

Table 1. Manufactured absorber test samples.

0EMD	1 × cement, 6 × sand
1EMD	1 × cement, 5 × sand, 1 × EMD
2EMD	1 × cement, 4 × sand, 2 × EMD
3EMD	1 × cement, 3 × sand, 3 × EMD
4EMD	1 × cement, 2 × sand, 4 × EMD
4.5EMD	1 × cement, 1.5 × sand, 4.5 × EMD
5EMD	1 × cement, 1 × sand, 5 × EMD
3CHY13K	1 × cement, 3 × sand, 3 × CHY13K
4CHY13K	1 × cement, 2 × sand, 4 × CHY13K
5CHY13K	1 × cement, 1 × sand, 5 × CHY13K

the attenuation, *R* the reflection loss and *B* the correction term due to successive reflections and attenuations internal to the material.

Measuring the transmission coefficient S_{21} between the two antennae with the DUT in the propagation path of the EMW, will reveal the SE of the material. The difference between the measured S_{11} as the reflection coefficient Γ, and S_{21} the SE, results in the attenuation. The absorption capability of the sample is determined from (1-Γ).

Measurement setup

The measurement setup used to measure total SE is shown in Figure 1. The setup consisted of a HP37269D VNA, and two ultra broadband open horn antennae (Bantsis et al., 2012). The transmit antenna (TX) used is a 500 MHz to 4 GHz double-ridged horn antenna, part number 470523 from Saab-Grintek Technologies. The receive antenna (RX) used is a model 3115 double-ridged waveguide horn antenna manufactured by ETS-Lindgren with a frequency range of 750 MHz to 18 GHz. The S_{21} parameter was measured with the VNA in an anechoic chamber to determine the transmission coefficient of the test samples.

With the setup for S_{11} measurements, only the TX antenna and the VNA was used, while S_{11} parameters of a conductive plate with the same dimensions as the absorber material was measured and used as a reference. The absorption and reflection loss of the material is then determined without a conducting back plate by measuring S_{11} and S_{21} of the absorbing material (Sagnard and El Zein, 2005).

The measurements were done in an anechoic chamber lined with Eccosorb AN absorption material operational for a 600 MHz - 40 GHz frequency range. The chamber is designed to reflect less than -20 dB of normal incident energy. The test setups were calibrated to ensure minimum VSWR and path loss. Traditional time domain reflectometry (TDR) is achieved by launching an impulse or step into the test device and observing the response in time with a wideband receiver. The transform used by a VNA resembles TDR; however, the VNA makes swept frequency response measurements and mathematically transforms the data into a TDR-like display. This is useful to determine impedance mismatches which are the main cause of reflection loss. The time domain gating function on the VNA allows selective removal of reflection or transmission responses. The data can then be converted to the frequency domain for analysis.

Measurements were done in the following frequency bands: GSM850: 824–894 MHz; GSM900: 890-960 MHz; GSM1800: 1.71-1.88 GHz; GSM1900: 1.86-1.99 GHz; WiFi: 2.4-2.484 GHz (Figure 2).

RESULTS AND DISCUSSION

The various samples in Table 1 were investigated and the 5EMD was analyzed in this research due to its superior performance. Figures 2 to 4 show the measured results. The total loss indicates the transmission loss determined by measuring S_{21}. The reflection loss and attenuation were determined from the S_{11} measurement. The transmission loss was calculated using Equation (6) and compared with measured results from 800 MHz to 2.8 GHz in Figure 5. The multiple internal reflections and attenuations were included in the measured attenuation.

The 5EMD sample had low reflection loss and very good absorption in the GSM850 and GSM900 mobile communication bands as indicated in Figure 2. For the GSM1800 and GSM1900 frequency bands the attenuation is lower at the higher frequency bands as shown in Figure 3. For the WiFi frequency band as shown in Figure 4, the attenuation was also lower when compared to Figure 2. Hence, this resulted in a lower SE.

Figure 5 shows good correlation between the measured results and calculated data. In Figure 6 the superior SE of EMD over MnZn-ferrite is clearly visible. Figure 6 also shows the increase of SE with the addition of EMD to the cement based composite.

Measuring the S11 parameter to determine the absorption and reflection capabilities and S_{21} parameter to determine the transmission loss of the material enabled the authors to determine the attenuation of the EMW in the material. The major advantage in using such a measurement technique is that one is able to distinguish between reflection loss, attenuation, absorption and transmission loss and this enables the researcher to manipulate these characteristics to improve the performance by adjusting the composite building material for EMW absorption and attenuation. The measured results in Figure 2 show that EMD can be used effectively in cement-based material to obtain a typical SE of 8dB. With the measured results shown in Figure 6, the authors also demonstrate in this research that the SE of plaster cement can be improved by adding EMD powder to its matrix to create a composite cement-based building

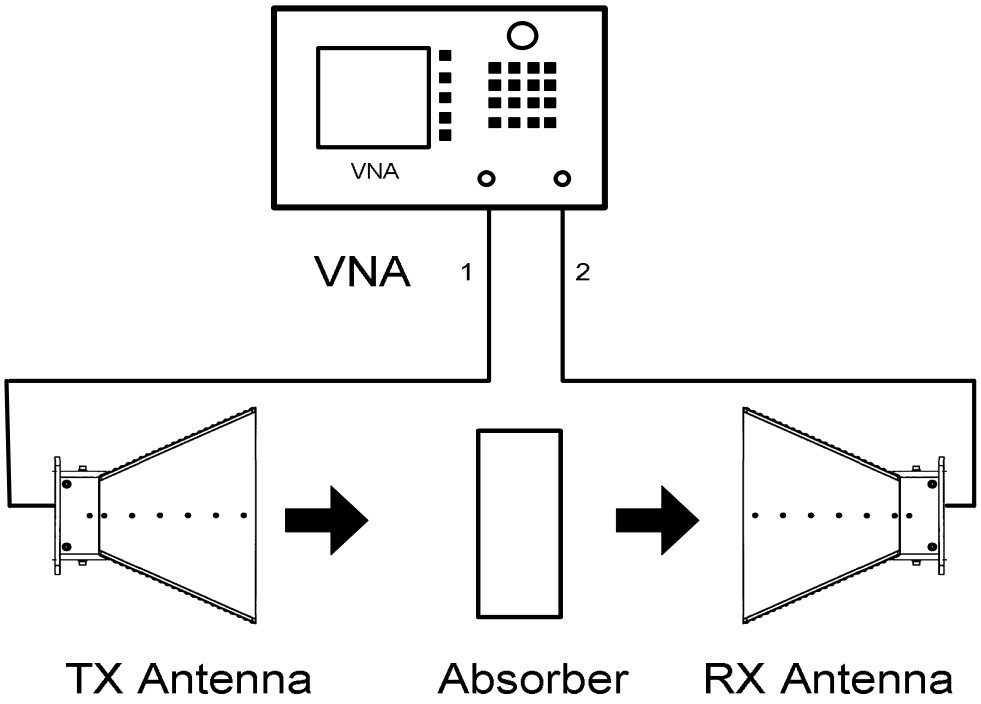

Figure 1. Measurement setup for determination of transmission loss (S_{21}).

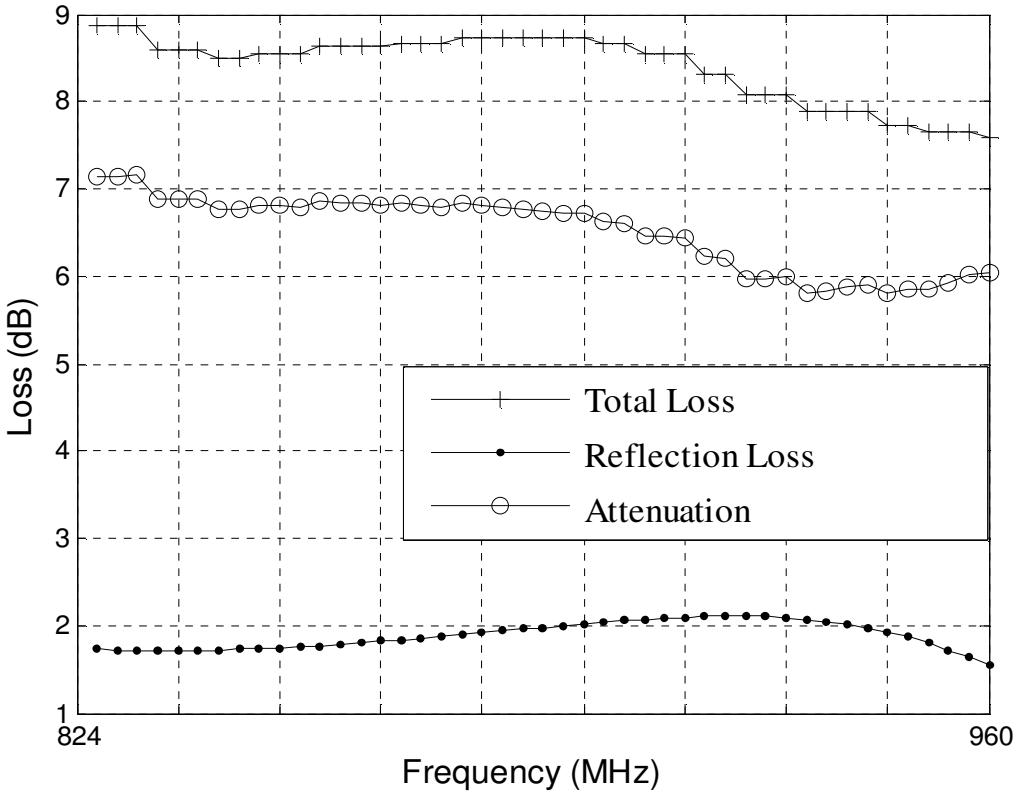

Figure 2. Measured results in the GSM850 and GSM900 frequency bands of the total loss (SE), attenuation and reflection loss.

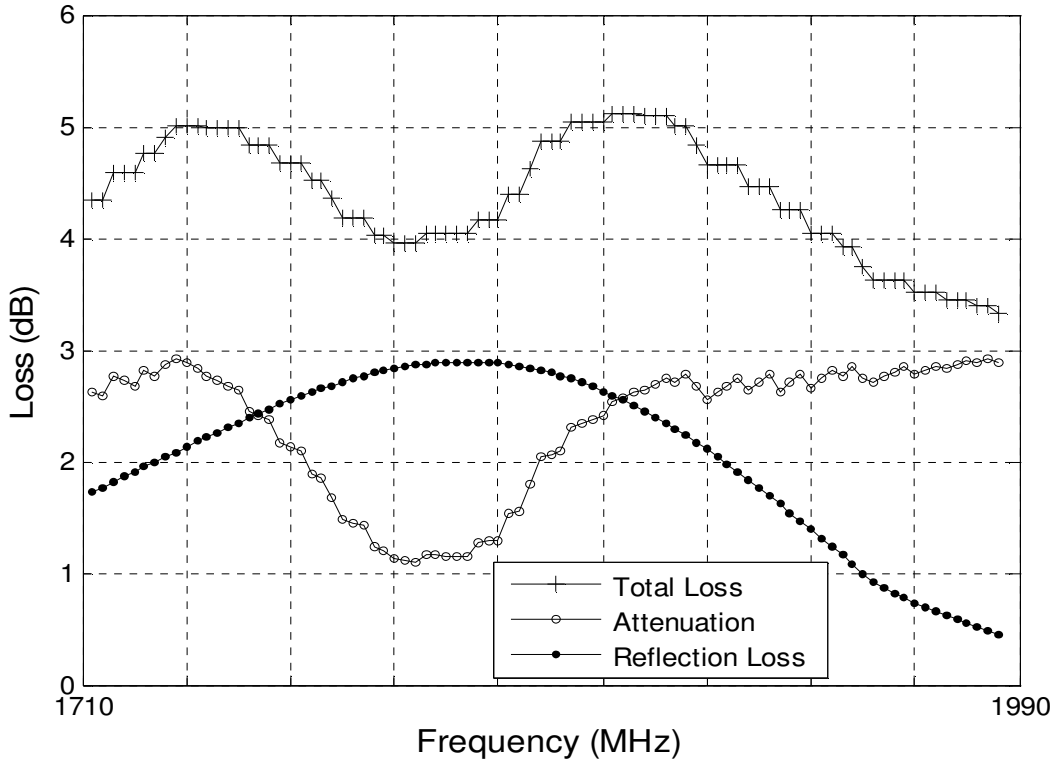

Figure 3. Measured results in the GSM1800 and GSM1900 frequency bands of the total loss (SE), attenuation and reflection loss.

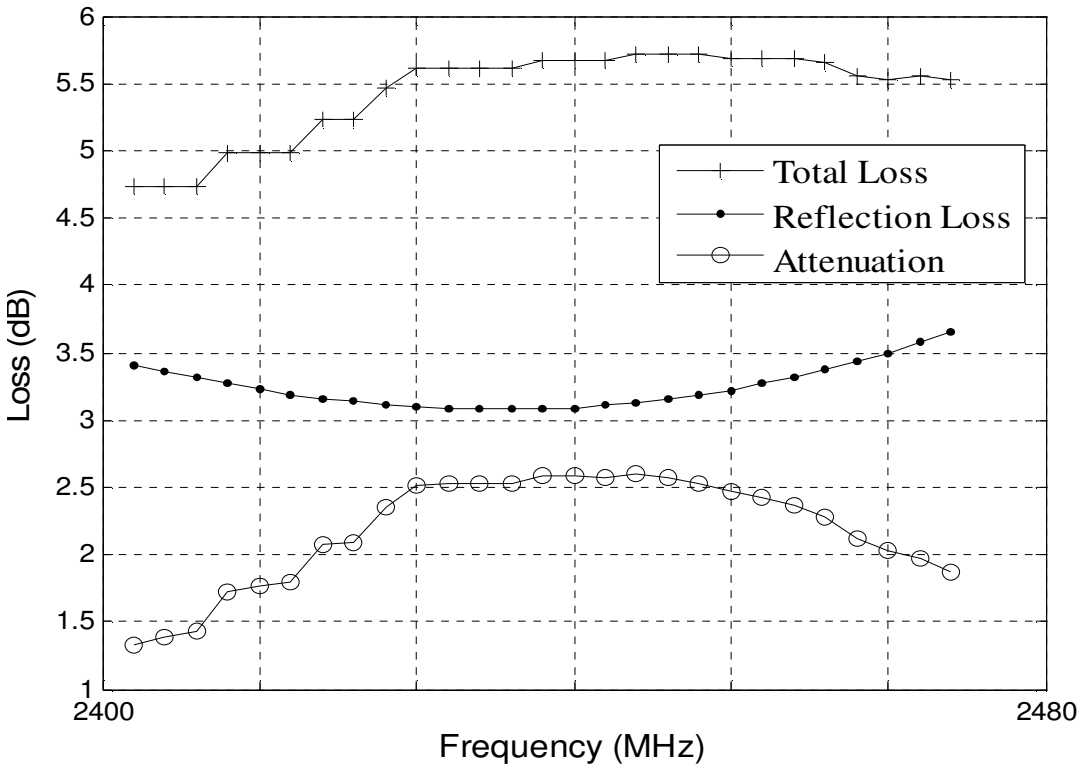

Figure 4. Measured results in the WiFi frequency band of the total loss (SE), attenuation and reflection loss.

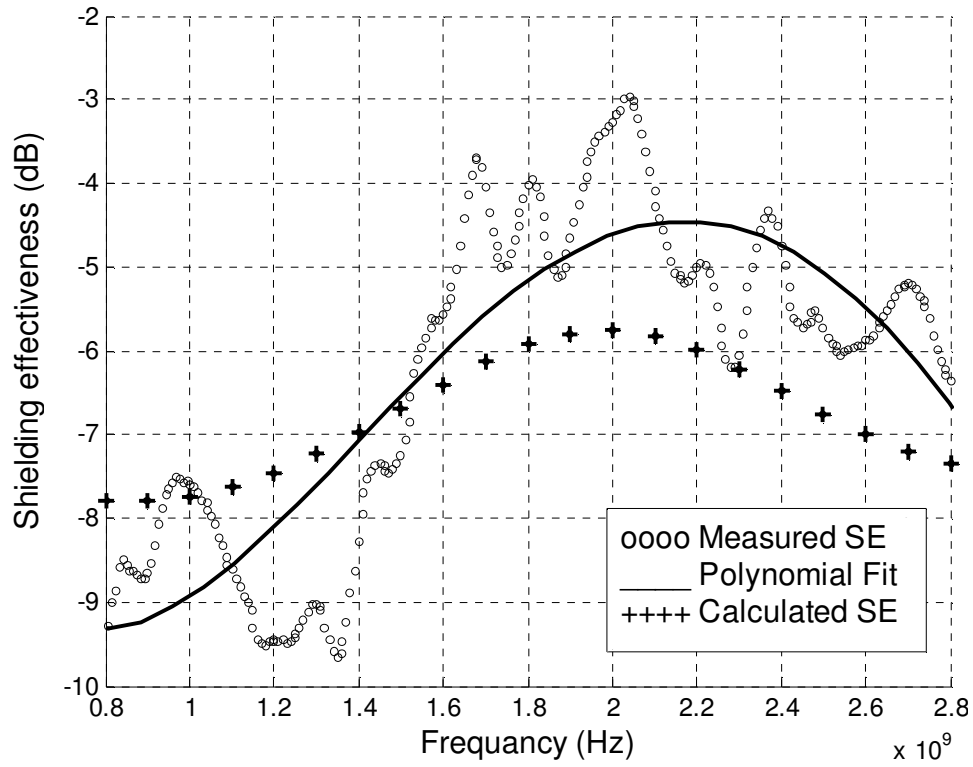

Figure 5. Comparison of measured results and calculated data of the transmission loss from 800 MHz to 2.8 GHz.

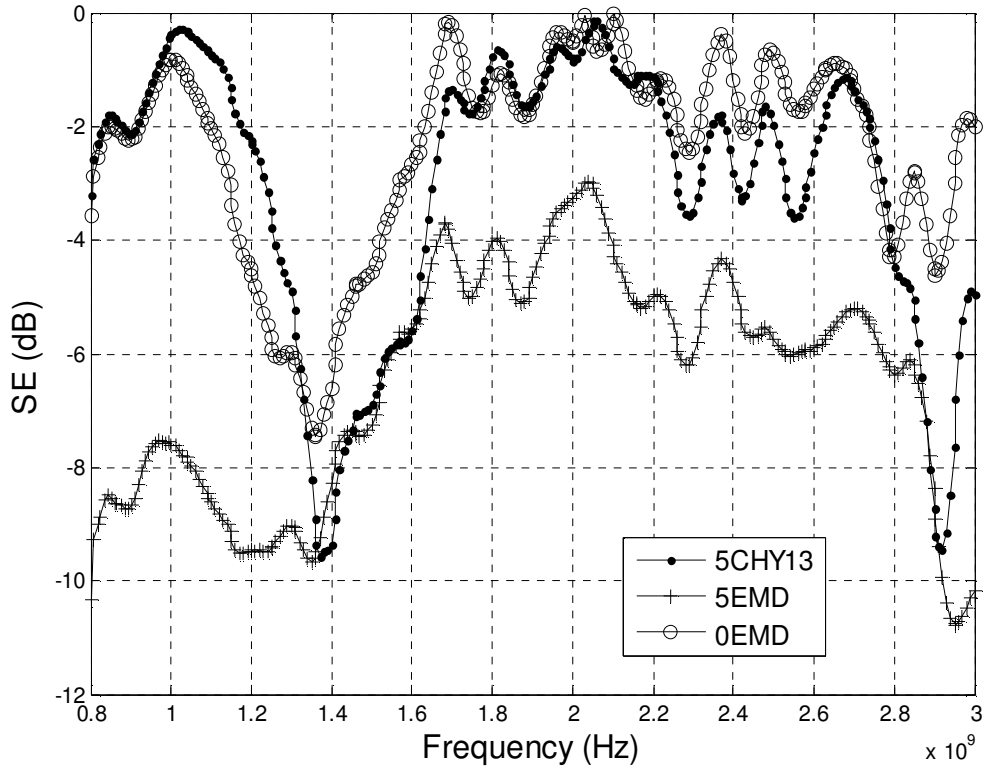

Figure 6. SE comparison of 0EMD, 5EMD and 5CHY13 samples.

material absorber. This new absorber material showed superior SE performance compared to the commonly used MnZn-ferrite.

Conclusion

It is believed that this composite cement-based material which the authors investigated and characterized in this research can practically be applied in a plaster cement form or as pre-manufactured tiles to shield priority indoor premises effectively from outside electromagnetic interference.

ACKNOWLEDGMENT

The authors wish to thank Saab-Grintek Technologies in Centurion, South Africa for the availability of their anechoic chamber and test equipment.

ABBREVIATIONS

EMW, Electromagnetic wave; **VNA,** vector network analyser; **SE,** shielding effectiveness; **DUT,** device under test; **EMD,** electrolytic manganese dioxide; **TX,** transmit; **RX,** receive; **TDR,** time domain reflectometry.

REFERENCES

Bantsis G, Mavridou S, Sikalidis C, Betsiou M, Oikonomou N, Yioultsis T (2012). Comparison of low cost shielding-absorbing cement paste building materials in X-band frequency range using a variety of wastes. Ceram. Int. Elsevier 3:3683-3692.

Baoyi L, Yuping D, Shunhua L (2012). The electromagnetic characteristics of fly ash and absorbing properties of cement-based composites using fly ash as cement replacement. Const. Build. Mater. Elsevier 27:184-188.

Guan H, Liu S, Duan Y (2005). Expanded polystyrene as an admixture in cement-based composite for electromagnetic absorbing. J. Mater. Eng. Perform. pp. 68-72.

Guan H, Liu S, Duan Y, Cheng J (2006). Cement based electromagnetic shielding and absorbing building material. Cement Concrete Compos. Elsevier 28:468-474.

Guan H, Liu S, Duan Y, Zhao Y (2007). Investigation of the electromagnetic characteristics of cement based composites filled with EPS. Cement Concrete Compos. Elsevier 29:49-54.

Hutagalung SD, Sahrol NH, Ahmad ZA, Ain MF, Othman M (2012). Effect of MnO_2 additive on the dielectric and electromagnetic interference shielding properties of sintered cement-based ceramics. Ceram. Int. Elsevier 38:671-678.

Kharkovsky SN, Akay MF, Hasar UC, Atis CD (2002). Measurement and monitoring of microwave reflection and transmission properties of cement-based specimens. IEEE Trans. Instr. Meas. 51(6):1210-1218.

Kim HM, Kim K, Lee CY, Joo J, Cho SJ, Yoon HS, Pejakovic DA, Yoo JW, Epstein AJ (2004). Electrical conductivity and electromagnetic interferance shielding of multiwalled carbon nanotube composites containing Fe catalyst. Appl. Phys. Lett. 84(4):589-591.

Mishra M, Singh AP, Dhawan SK (2013). Expanded graphite-nanoferrite-fly ash composites for shielding of electromagnetic pollution. J. Alloys Compd. Elsevier 557:244-251.

Nie Y, He H, Feng Z, Xiong B (2005). Absorbing properties of the magnetic composite electromagnetic wave absorber. Proc. IEEE Int. Symp. Microwave, Antenna, Propagation and EMC Technologies for Wireless Communications, Beijing, China, 8-12 August, 2005, pp. 724-727.

Oka H, Tanaka K, Osada H, Kubota K, Dawson FP (2009). Study of electromagnetic wave absorption characteristics and component parameters of laminated-type magnetic wood with stainless steel and ferrite powder for use as building materials. J. Appl. Phys. 105:1-3.

Park KY, Lee SE, Kim CG, Han JH (2006). Fabrication and electromagnetic characteristics of electromagnetic wave absorbing sandwich structures. Compos. Sci. Technol. Elsevier 66:576-584.

Sagnard F, El Zein G (2005). Characterization of building materials for propagation modeling: Frequency and time response. Int. J. Electron. Comm. Elsevier 59:337-347.

Schulz RB, Plantz VC, Brush DR (1988). Shielding theory and practice. IEEE Trans. Electromagn. Compatibility 30(3):187-200.